BO_3 MOLECULAR STRUCTURES: EXAMPLES OF THE IMPORTANCE OF ELECTRON CORRELATION

Alexander Yu. SOKOLOV[1], Nathan J. STIBRICH[2] and Henry F. SCHAEFER III[3,*]

Center for Computational Quantum Chemistry, University of Georgia, Athens, Georgia 30602, U.S.A.; e-mail: [1] alex@ccqc.uga.edu, [2] stibrich@gmail.com, [3] sch@uga.edu

Received August 22, 2008
Accepted August 27, 2008
Published online December 1, 2008

Dedicated to Professor Rudolf Zahradník on the occasion of his 80th birthday.

In 1991 Burkholder and Andrews reported the spectroscopic identification of the boron–oxygen species BO, BO_2, B_2O_2, B_2O_3, and BO_2^-. In addition, they tentatively identified two infrared features due to BO_3. In this research, a wide range of possible BO_3 structures is considered theoretically. The highest level of theory used involves the CCSD(T) method with an augmented correlation consistent quadruple zeta basis set. A planar structure O–B–O–O is predicted to be the global minimum, lying 4.2 kcal mol^{-1} below a higher symmetry (C_{2v}) structure incorporating a BO_2 isosceles triangle. Reasonable agreement is found between the theoretical vibrational frequencies and the two fundamentals reported by Burkholder and Andrews. The potentially important ozone adduct B–O_3 is predicted to lie much higher in energy.

Keywords: Boron oxides; IR spectroscopy; *Ab initio* calculations; CCSD(T) method.

The extreme exothermicity of reactions involving boron-containing species and oxygen has made boron compounds a significant target for new fuels. For these purposes it is important to understand the nature of boron combustion processes, as well as their thermodynamic and kinetic properties. A variety of experimental physical methods have been applied in order to investigate the gas phase compositions of boron containing mixtures at high temperatures[1–4].

Numerous experimental studies in the 1950s and 1960s made important contributions to the understanding of the boron combustion chemistry. Using a combination of the Knudsen effusion method and mass-spectrometric techniques, the vapor accompanying B–B_2O_3 mixtures was found to consist mainly of B_2O_3 and B_2O_2 in the 1300–1500 K temperature range[1].

Collect. Czech. Chem. Commun. 2008, Vol. 73, No. 11, pp. 1495–1508

doi:10.1135/cccc20081495

Later, infrared emission studies of B_2O_3 and B_2O_2 were used to determine the structures of these species, though there was some dispute over the B_2O_3 structure[5,6]. Matrix isolation infrared absorption investigations of high-temperature B_2O_3 and B_2O_2 were performed to trap these hot vapor species in a cold inert gas matrices (~20 K), in order to obtain their vibrational spectra[2,3]. These studies confirmed the V-shaped structure of B_2O_3 proposed in ref.[6]. The linearity of B_2O_2 was confirmed by photoelectron spectroscopy[4].

While B_2O_3 and B_2O_2 are closed-shell molecules, several radical forms of B,O-containing compounds have also been detected in the gas phase. Direct reaction of the boron atoms with oxygen in the gaseous phase primarily produces the BO radical[7]. The BO_2 radical was first observed by means of electron spectroscopy in a BCl_3/O_2 flash photolysis study[8], and it was shown that the molecule has a linear structure. This conclusion was also confirmed by infrared spectroscopic studies[3].

Numerous researchers[9–13] have shown the usefulness of matrix infrared spectroscopy applied to boron compounds in high-temperature vapor. The combination of this experimental technique with theoretical calculations often enables one to accurately determine the structures of the species. Due to their transient nature and small number of electrons, high quality quantum chemical calculations are well-suited for studies of oxyboron compounds. To date, a number of important theoretical studies of B,O-containing molecules have been reported[14–20].

It is now clear that BO_2 forms as the result of the BO radical oxidation process:

$$BO + O_2 \Rightarrow BO_2 + O \, .$$

The kinetic and thermodynamic properties of this reaction have been thoroughly investigated by several authors[21–23]. Nevertheless, the detailed mechanism of this process, which is one of the key reactions in boron combustion[22], is still unknown. It was thought by earlier researchers that the BO_2 radical is produced as the result of a simple oxygen atom transfer from O_2 molecule to BO. However, the negative temperature dependences of the reaction rate constant persuaded Oldenborg and Baughcum[23] to assume the formation of the BO_3 intermediate. Stanton and co-workers[24] drew the same conclusion about the mechanism of this reaction on the basis of laser-induced fluorescence measurements. In Stanton's work, results of SCF/CI calculations were also presented, where the BO_3 radical was qualitatively considered as a C_{2v} symmetry molecule with a cyclic OBO fragment. How-

ever, the importance of this reaction certainly warrants further theoretical study.

The main goal of the present study is to determine the most probable structures of the BO_3 intermediate and thus make an important step in elucidating the mechanism of BO oxidation reactions. We also aimed to predict the dissociation energies of the lowest-lying BO_3 structure to two sets of products: (*1*) BO and O_2, (*2*) BO_2 and O. To this end we have applied reliable quantum mechanical methods to various possible BO_3 structures.

METHODS

For the initial evaluation of the relative energies of the species, the restricted open-shell Hartree–Fock (ROHF) method was used. A detailed study of BO_3 radical structures was then carried out using single-reference unrestricted coupled-cluster UCCSD and UCCSD(T) methods. Both of these methods incorporate single and double excitations, the latter also perturbatively including connected triple excitations. These methods have proven to be very reliable for the highly accurate determination of structures and energies.

For all atoms the correlation-consistent aug-cc-pVXZ (X = D, T and Q) basis sets developed by Dunning and co-workers were used[25–27]. All computations were performed using the MOLPRO 2006.1 computational quantum chemistry package[28]. For the B and O atoms, 1s orbitals have been frozen in all treatments of electron correlation. Although MOLPRO uses an unrestricted coupled cluster formulation, the orbitals employed throughout are ROHF orbitals.

In the computations the geometries of all structures were fully optimized. Vibrational frequencies were evaluated to determine the Hessian index of each stationary point. Geometry optimization and harmonic vibrational frequency analysis were performed by numerical differentiation of the potential energy, with gradients and energies converged to 10^{-8} and 10^{-10} a.u., respectively.

RESULTS AND DISCUSSION

Preliminary Computations

Utilizing ROHF theory with the aug-cc-pVDZ basis sets, several possible structures for the BO_3 radical were optimized. For all structures vibrational frequencies were computed to determine the character of the stationary

points. The structures along with their total energies are given in Table I. To determine the most probable structures of the BO_3 radical, two main criteria have been taken into account: (i) the true local minimum character of the stationary point (absence of imaginary frequencies) and (ii) a comparatively low energy. On the basis of these criteria, structures **I–III** (Table I) were chosen for further investigation.

TABLE I

Types of BO_3 radical structures, symmetries of the molecules, multiplicities (D, doublet; Q, quartet), characters of the stationary points and energies (*E*) computed at the ROHF/aug-cc-pVDZ level of theory (energies for the highest of considered level of theory are given in parenthesis). All structures are planar

Type	Structure	Sym. (Mult.)	Stationary point character	*E*, a.u.
I[a]	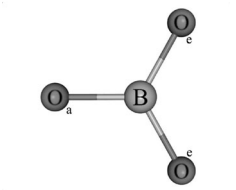	D_{3h} or C_{2v} (Q)	minimum	–249.29278 (–250.13898)
II	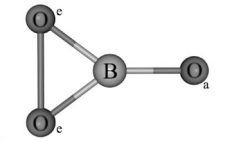	C_{2v} (D)	minimum	–249.22646 (–250.16705)
III	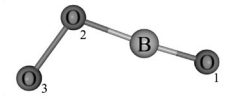	C_s (D)	minimum	–249.23928 (–250.17371)
IV	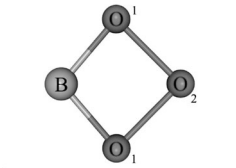	C_{2v} (D)	minimum	–249.09221
V		$C_{\infty v}$ (D)	dissociates to $BO + O_2$	–
VI		$C_{\infty v}$ (D)	transition state	–
VII		C_s (D)	transition state	–

[a] Due to the MOLPRO limitations the symmetry group for structure **I** was specified as C_{2v}. Therefore electronic states and vibrational frequences are interpreted in terms of irreducible representations of this point group.

*Structures **I–III***

For structures **I–III** the geometries of the lowest energy state of each symmetry type were optimized in the framework of the ROHF and UCCSD methods. Computations were initially carried out using aug-cc-pVDZ basis set. These results are reported in Tables II and III. For all structures doublet and quartet spin states were considered. Structure **I** is found to have three unpaired elec- trons in its ground $^4A_1$ state, while the ground states of structures **II** and **III** are of $^2B_2$ and $^2A''$ symmetry, respectively. Quartet states of structures **II** and **III** possess very high energies and tend to dissociation or collapse to structure **I**. For this reason these quartet states will not be considered further.

Geometry optimization of structure **I** for all electronic states except $^2A_1$ and $^4A_1$ leads to structure **II** or dissociation. With the ROHF/aug-cc-pVDZ method (Tables II and III) structure **I** is the global minimum on the $^4A_1$ potential energy surface. The ROHF $^2A''$ state of structure **III** is predicted to lie 34 kcal mol^{-1} higher in energy, being the second lowest (Fig. 1). Structures **II** and **III** are rather close energetically, with a difference of only 8 kcal mol^{-1}.

Structure **III**'s ground and excited state geometries differ slightly (Table III). For structures **I** and **II** the situation is more complicated. The $^2B_2$, $^2B_1$, and $^2A_1$ excited states differ in geometry only minimally. The lowest $^2A_2$ state, however, differs drastically, with a significant increase in the (O_a–B–O_e) angle and stretching of the B–O_e bond length (Table II) accompanied by shortening of B–O_a distance. This structure proves to be a transition state leading to dissociation and has an imaginary vibrational frequency of 1905 i cm^{-1}. Geometry optimization of the structure **I** $^2A_1$ excited state collapses to the structure **II** electronic state of the same symmetry.

In Tables II and III results of UCCSD/aug-cc-pVDZ computations for three structures are presented. The results at this level of theory differ radically from those obtained by the ROHF/aug-cc-pVDZ method, illustrating the importance of electron correlation for an accurate description of these systems. The structure **I–III** ground states are found to be the same, but these states are much closer in energy. Comparative analysis of the results in Tables II and III shows that structure **III** now has the lowest energy. The ground state of structure **II** lies 7.2 kcal mol^{-1} higher in energy, while structure **I** is 12.6 kcal mol^{-1} above structure **III**. Figure 1 reflects these results in comparison to results obtained at the lower level of theory.

Inclusion of electron correlation does not greatly affect the geometrical parameters of the structures. Bond lengths do increase by about 0.01–0.04 Å compared to ROHF/aug-cc-pVDZ results. For the ground and excited states

TABLE II

Energies, geometrical parameters and vibrational frequencies for the various electronic states of structures **I** and **II** computed using the two initially adopted levels of theory. The lowest energy states for each structure and level of theory are given in bold

State	*E* a.u.	r(B–O_a) Å	r(B–O_e) Å	∠(O_a–B–O_e) °	ω(a_1) cm^{-1}	ω(b_1) cm^{-1}	ω(b_2) cm^{-1}
			Structure I				
			ROHF/aug-cc-pVDZ				
$^2A_1$			Optimization leads to structure **II** $^2A_1$ state				
$^4A_1$	**–249.29278**	**1.370**	**1.370**	**120.0**	**1415, 895 442**	**689**	**1415 442**
			UCCSD/aug-cc-pVDZ				
$^2A_1$	–249.85175	1.389	1.386	119.1	1304, 830 377	634	1304 282
$^4A_1$	**–249.85817**	**1.389**	**1.389**	**120.0**	**1243, 835 404**	**624**	**1243 404**
			Structure II				
			ROHF/aug-cc-pVDZ				
$^2A_1$	–249.11329	1.340	1.326	144.3	1761, 982 708	534	1122 480
$^2A_2$	–249.19487	1.203	1.473	153.7	2064, 1373 797	534	*1904i* 489
$^2B_1$	–249.21090	1.374	1.328	144.6	1821, 995 717	522	1062 460
$^2B_2$	**–249.22646**	**1.343**	**1.332**	**145.0**	**1842, 1005 725**	**541**	**1095 424**
			UCCSD/aug-cc-pVDZ				
$^2A_1$			Optimization leads to structure **I** $^2A_1$ state				
$^2A_2$	–249.86331	1.230	1.513	152.7	1914, 1107 716	481	449 193
$^2B_1$	–249.85038	1.394	1.359	142.0	1643, 873 536	497	1091 410
$^2B_2$	**–249.86683**	**1.353**	**1.366**	**143.1**	**1620, 888 551**	**514**	**1059 369**

TABLE III

Energies, geometrical parameters and vibrational frequencies for $^2A'$ and $^2A''$ electronic states of structure **III** computed using the two initially adopted levels of theory. The lowest energy states for each level of theory are given in bold

State	*E* a.u.	$r(O_1–B)$ Å	$r(B–O_2)$ Å	$r(O_2–O_3)$ Å	$\angle(O_1–B–O_2)$ °	$\angle(B–O_2–O_3)$ °	ω(a′) cm^{-1}	ω(a″) cm^{-1}
				ROHF/aug-cc-pVDZ				
$^2A'$	–249.22782	1.190	1.337	1.354	178.1	114.3	2212 1240 949 639 233	548
$^2A''$	**–249.23928**	**1.188**	**1.350**	**1.332**	**177.4**	**111.1**	**2213** **1226** **977** **634** **243**	**530**
				UCCSD/aug-cc-pVDZ				
$^2A'$	–249.86106	1.217	1.364	1.401	177.3	110.8	2055 1064 837 566 204	500
$^2A''$	**–249.87835**	**1.214**	**1.385**	**1.371**	**176.4**	**105.8**	**2051** **1068** **897** **544** **216**	**473**

of structure **II**, UCCSD decreases the O_a–B–O_e angle by about 2°. The same tendency can also be found for the O_1–B–O_2 and B–O_2–O_3 angles of structure **III**.

Vibrational frequency analysis shows that the $^2A_2$ excited state of structure **II** is a true minimum with a comparatively long B–O_e bond length of 1.513 Å. The presence of the low frequency vibration (192 cm^{-1}) in the vibrational spectrum may be attributed to the weak chemical interactions between these atoms. In contrast to the ROHF/aug-cc-pVDZ results, the $^2A_2$ excited state is much closer to the ground state than $^2B_1$. This circumstance is attributed to the importance of the electron correlation for describing weak interactions.

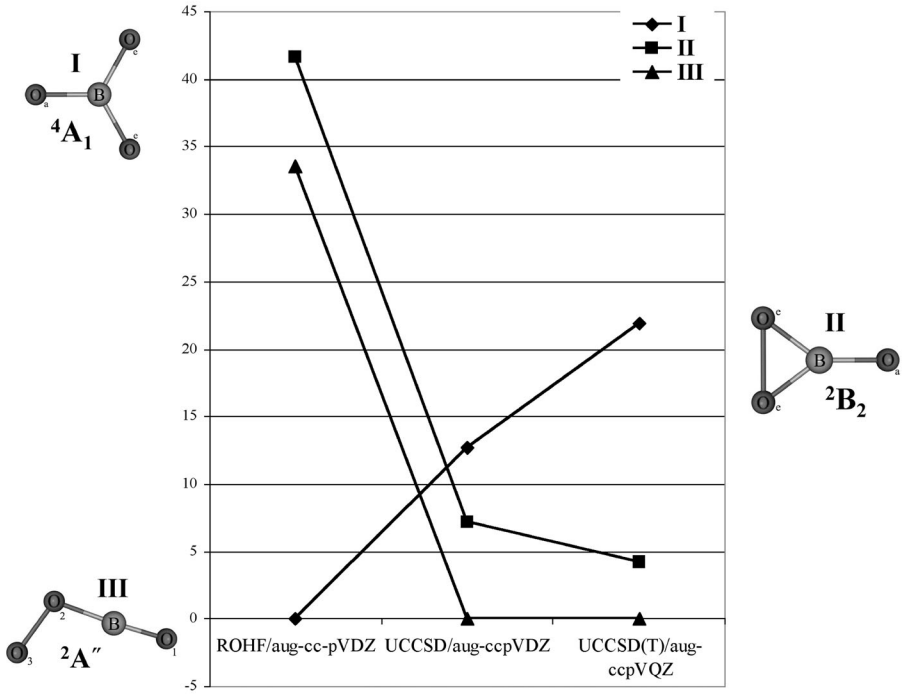

FIG. 1

Relative energies (in kcal mol^{-1}) of the structures **I**, **II**, and **III** ground states computed using three different levels of theory. The energy of the lowest-lying structure is considered as zero energy level

*More Concerning Structures **II** and **III***

According to the UCCSD/aug-cc-pVDZ results, the most probable geometry for the BO_3 radical is structure **III**. Two of the lower lying electronic states, the $^2A''$ state of structure **III** and the $^2B_2$ state of structure **II**, were chosen for a more accurate investigation using high levels of theory. For these purposes we used the UCCSD and UCCSD(T) methods with the aug-cc-pVXZ (X = D, T, Q) correlation-consistent basis sets. Results of these higher level computations are given in Tables IV and V.

Tables IV and V allow one to compare energies, geometries and harmonic vibrational frequencies of the structures **II** and **III** ground states between six different levels of coupled cluster theory. The following regularities should

TABLE IV
Energies, geometrical parameters and vibrational frequencies for the $^2B_2$ electronic state of structure **II** computed using six different levels of coupled cluster theory

Method	*E* a.u.	r(B–O_a) Å	r(B–O_e) Å	∠(O_a–B–O_e) °	ω(a_1) cm^{-1}	ω(b_1) cm^{-1}	ω(b_2) cm^{-1}
			aug-cc-pVDZ				
UCCSD	–249.86683	1.353	1.366	143.1	1620 888 551	514	1059 369
UCCSD(T)	–249.89359	1.356	1.374	142.0	1568 862 459	510	1046 358
			aug-cc-pVTZ				
UCCSD	–250.06677	1.343	1.353	143.8	1683 931 604	508	1106 372
UCCSD(T)	–250.10360	1.344	1.360	142.9	1625 903 522	502	1090 360
			aug-cc-pVQZ				
UCCSD	–250.12784	1.338	1.347	143.8	1688 937 612	510	1108 373
UCCSD(T)	–250.16705	1.339	1.355	143.0	1630 908 531	503	1092 360

TABLE V
Energies, geometrical parameters and vibrational frequencies for the $^2A''$ electronic state of structure **III** computed using six different levels of coupled cluster theory

Method	*E* a.u.	$r(O_1–B)$ Å	$r(B–O_2)$ Å	$r(O_2–O_3)$ Å	$\angle(O_1–B–O_2)$ °	$\angle(B–O_2–O_3)$ °	ω(a′) cm^{-1}	ω(a″) cm^{-1}
				aug-cc-pVDZ				
UCCSD	–249.87835	1.214	1.385	1.371	176.4	105.8	2051, 1068 897, 544 216	473
UCCSD(T)	–249.90268	1.221	1.384	1.389	176.3	104.6	2006, 1018 880, 520 209	459
				aug-cc-pVTZ				
UCCSD	–250.07416	1.207	1.373	1.357	176.6	106.9	2096, 1123 929, 543 209	471
UCCSD(T)	–250.10941	1.214	1.377	1.370	176.5	105.5	2049, 1075 913, 517 201	457
				aug-cc-pVQZ				
UCCSD	–250.13612	1.201	1.368	1.350	176.7	107.2	2110, 1140 934, 548 210	472
UCCSD(T)	–250.17371	1.208	1.373	1.362	176.6	105.8	–	–

be noted: (i) inclusion of the connected triple excitations leads to the slight stretching of the bond lengths, while decreasing the bond angles and vibrational frequencies; (ii) increasing of the size of the basis set affects these parameters in the opposite direction: shortens the bond lengths, increases the angles and vibrational frequencies. The overall changes of the geometry and vibrational frequencies between the lowest (UCCSD/aug-cc-pVDZ) and the highest (UCCSD(T)/aug-cc-pVQZ) levels of theory consist of a small shortening of the bond lengths, almost constant values of bond angles, and higher vibrational frequencies.

All levels of theory (Table V) predict structure **III** ($^2A''$ state) to be the global minimum of the BO_3 radical. The energy difference between this state and the $^2B_2$ state of structure **II** decreases after the addition of the connected triple excitations component to only 4.2 kcal mol^{-1} at the highest level of theory (Fig. 1).

Ground state geometries for structures **I**, **II**, and **III** computed at UCCSD(T)/aug-cc-pVQZ, our highest level of theory, are presented in Figs 2–4. B–O_a and B–O_e bond lengths of the structure **II** ground state are similar with a difference of 0.016 Å. These bonds are quite long in comparison to B–O bond lengths known in literature and are nearly 0.1 Å longer than in BO_2 radical (experimental value is 1.265 Å). The O_e–O_e bond distance is very long, 0.158 Å longer than the already long oxygen–oxygen bond in hydrogen peroxide (1.475 Å). The B–O bond lengths of the structure **III** ground state are very different. Similar to the B–O distance in boron monoxide (1.205 Å), the B–O_1 (1.208 Å) bond is much shorter than B–O_2 (1.373 Å). The O_2–O_3 bond distance (1.362 Å) is intermediate between the double bond in O_2 molecule (1.208 Å) and the single bond in H_2O_2.

A matrix isolation infrared study of the B,O-containing vapor was carried out by Burkholder and Andrews[29]. The experimental IR frequencies depend on matrix isolation conditions and boron and oxygen isotope compositions. Their infrared spectra contain several IR bands, which were attributed to the unidentified OBOX (2119 cm^{-1}; 2113 cm^{-1}) and OBOY (2081 and 513 cm^{-1}; 2076 cm^{-1}; 2077 and 513 cm^{-1}) species[+]. In the note added in proof of the Burkholder–Andrews paper these species were tentatively identified as OBOB and OBOO molecules. The theoretical vibrational frequencies (2049 and 517 cm^{-1}, UCCSD(T)/aug-cc-pVTZ) for the lowest-lying structure **III** ground state are in reasonable agreement with the two observed frequen-

+ Results for $^{10}B/^{16}O_2$ system only are mentioned in the text.

cies for the OBOY species and serve as a confirmation of the tentative Burkholder–Andrews identification of BO_3. It is worthwhile to mention that the 1682 cm^{-1} IR band unidentified in ref.[29] is very close to one of the theoretical vibrational frequencies for the ground state of the second-lowest structure **II** (1630 cm^{-1} (a_1), UCCSD(T)/aug-cc-pVQZ level).

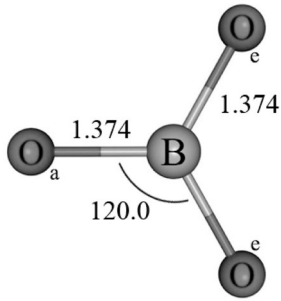

FIG. 2
Structure **I** $^4A_1$ ground state and its geometrical parameters optimized using the UCCSD(T)/aug-cc-pVQZ method. Bond lengths are given in Å, bond angle in °

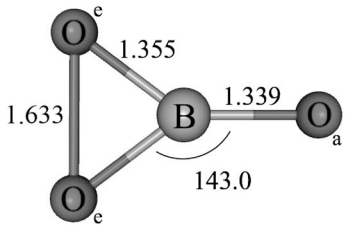

FIG. 3
Structure **II** $^2B_2$ ground state and its geometrical parameters optimized using the UCCSD(T)/aug-cc-pVQZ method. Bond lengths are given in Å, bond angle in °

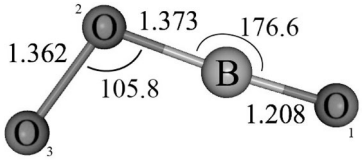

FIG. 4
Structure **III** $^2A''$ ground state and its geometrical parameters optimized using the UCCSD(T)/aug-cc-pVQZ method. Bond lengths are given in Å, bond angles in °

Bond Dissociation Energies

Theoretical dissociation energies (D_e) for the BO_3 radical (structure **III** $^2A''$ state) to two sets of products were predicted. For this purpose, absolute energies of the BO, O_2, and BO_2 molecules and the O atom were also computed at the same level of theory (Table VI). From the UCCSD(T)/aug-cc-pVQZ method for reaction (*1*) $BO_3 \Rightarrow BO + O_2$, D_e is predicted to be 58.5 kcal mol^{-1}. For reaction (*2*) $BO_3 \Rightarrow BO_2 + O$, D_e is 48.0 kcal mol^{-1}. Theoretical dissociation energies D_e for these reactions may be corrected by zero-point vibrational energies (ZPVEs) using computed vibrational frequencies. For the two processes ZPVE corrections reduce the dissociation energies by 2.5 and 2.8 kcal mol^{-1}, respectively, at the UCCSD(T)/aug-cc-pVTZ level of theory.

TABLE VI
Absolute energies (E) for BO, BO_2, BO_3, O, and O_2 species and bond dissociation energies (D_e) for two reactions computed on the UCCSD(T)/aug-cc-pVQZ level of theory

$BO_3 \Rightarrow BO + O_2$		$BO_3 \Rightarrow BO_2 + O$	
Molecule	*E*, a.u.	Molecule	*E*, a.u.
BO_3	–250.17371	BO_3	–250.17371
BO	–99.90181	BO_2	–175.10206
O_2	–150.17863	O	–74.99513
D_e = 58.5 kcal mol^{-1}		D_e = 48.0 kcal mol^{-1}	

CONCLUSIONS

Using the high-level UCCSD and UCCSD(T) quantum mechanical methods with large correlation-consistent basis sets, structures and energetics for the BO_3 radical have been predicted. It is demonstrated that the alternative C_{2v} structure **II** for this molecule is very close in energy to the C_s global minimum structure **III**. Comparative analysis of the results between the ROHF and UCCSD methods shows the importance of accounting for electron correlation in this system. Predicted vibrational frequencies are in good accord with available experimental values.

This research was supported by the Combustion Program, Basic Energy Sciences, U. S. Department of Energy.

REFERENCES

1. Inghram M. G., Porter R. F., Chupka W. A.: *J. Chem. Phys*. **1956**, *25*, 498.
2. Weltner W., Warn J. R.: *J. Chem. Phys*. **1962**, *37*, 292.
3. Sommer A., White D., Linnevsky M. J., Mann D. E.: *J. Chem. Phys*. **1963**, *38*, 87.
4. Ruscic B. M., Curtiss L. A., Berkowitz J.: *J. Chem. Phys*. **1984**, *80*, 3962.
5. Dows D. A., Porter R. F.: *J. Am. Chem. Soc*. **1956**, *78*, 5156.
6. White D., Walsh P., Mann D. E.: *J. Chem. Phys*. **1958**, *28*, 508.
7. Hanner A. W., Gole J. L.: *J. Chem. Phys*. **1980**, *73*, 5025.
8. Johns J. W. C.: *Can. J. Phys*. **1961**, *39*, 1738.
9. Ruatta S. A., Hintz P. A., Anderson S. L.: *J. Chem. Phys*. **1991**, *94*, 2833.
10. Burkholder T. R., Andrews L.: *J. Phys. Chem*. **1992**, *96*, 10195.
11. Burkholder T. R., Andrews L.: *Chem. Phys. Lett*. **1992**, *199*, 455.
12. Burkholder T. R., Andrews L., Bartlett R. J.: *J. Phys. Chem*. **1993**, *97*, 3500.
13. Zhou M., Jiang L., Xu Q.: *Chem. Eur. J*. **2007**, *10*, 5817.
14. Dewar M. J. S., Jie C., Zoebisch E. G.: *Organometallics* **1988**, *7*, 513.
15. Page M.: *J. Phys. Chem*. **1989**, *93*, 3639.
16. Martin J. M. L., François J. P., Gijbels R.: *Chem Phys. Lett*. **1992**, *193*, 243.
17. Nemukhin A. V., Weinhold F.: *J. Chem. Phys*. **1993**, *98*, 1329.
18. Drummond M. L., Meunier V., Sumpter B. G.: *J. Phys. Chem. A* **2007**, *111*, 6539.
19. Zhai H.-J., Li S.-D., Wang L.-S.: *J. Am. Chem. Soc*. **2007**, *129*, 9254.
20. Li S.-D., Zhai H.-J., Wang L.-S.: *J. Am. Chem. Soc*. **2008**, *130*, 2573.
21. Llewellyn I. P., Fontijn A., Clyne M. A. A.: *Chem. Phys. Lett*. **1981**, *84*, 504.
22. Yetter R. A., Rabitz H., Dryer F. L., Brown R. C., Kolb C. E.: *Combust. Flame* **1991**, *83*, 43.
23. Oldenborg R. C., Baughcum S. L.: *Advances in Laser Science I; AIP Conference Proceedings 146* (W. C. Stwalley and M. Lapp, Eds), p. 562. AIP, New York 1986.
24. Stanton C. T., Garland N. L., Nelson H. H.: *J. Phys. Chem*. **1991**, *95*, 8741.
25. Dunning T. H.: *J. Chem. Phys*. **1989**, *90*, 1007.
26. Kendall R. A., Dunning T. H., Harrison R. J.: *J. Chem. Phys*. **1992**, *96*, 6796.
27. Woon D. E., Dunning T. H.: *J. Chem. Phys*. **1993**, *98*, 1358.
28. Werner H.-J., Knowles P. J., Lindh R., Manby F. R., Schutz M., and others: *MOLPRO*, version 2006.1, a package of *ab initio* programs, see http://www.molpro.net.
29. Burkholder T. R., Andrews L. J.: *J. Chem. Phys*. **1991**, *95*, 8697.